

Nonequilibrium Campbell length: probing the vortex pinning potential

R. Prozorov and R. W. Giannetta

Loomis Laboratory of Physics, University of Illinois at Urbana-Champaign, 1110 West Green Street, Urbana, Illinois 61801.

T. Tamegai

Department of Applied Physics, The University of Tokyo, Hongo, Bunkyo-ku, Tokyo, 113-8656, Japan.

P. Guptasarma and D. G. Hinks

Chemistry and Materials Science Division, Argonne National Laboratory, Argonne, Illinois 60439.

(Submitted April 4, 2000)

The AC magnetic penetration depth $\lambda(T, H, j)$ was measured in presence of a macroscopic DC (Bean) supercurrent, j . In single crystal BSCCO below approximately 28 K, $\lambda(T, H, j)$ exhibits thermal hysteresis. The irreversibility arises from a shift of the vortex position within its pinning well as j changes. It is demonstrated that below a new irreversibility temperature, the nonequilibrium Campbell length depends upon the ratio j/j_c . $\lambda(T, H, j)$ increases with j/j_c as expected for a non-parabolic potential well whose curvature decreases with the displacement. Qualitatively similar results are observed in other high- T_c and conventional superconductors.

PACS numbers: 74.25.Nf, 74.60.Ec, 74.60.Ge

The AC penetration depth λ is an extremely sensitive probe of the vortex state. Models for the small-amplitude AC response usually assume a uniform distribution of vortices and a parabolic effective potential well [1–6]. However, experiments often probe a nonequilibrium flux profile. In this case, λ may depend not only upon H and T but also upon the Bean supercurrent j arising from a gradient of vortex density. In this paper we show that a finite j produces a hysteretic AC response whenever the pinning potential is non-parabolic. In contrast to most experiments, the irreversibility discussed here occurs with temperature while the applied field is held constant. Thermal hysteresis is observed in several materials, but we focus on BSCCO. In all our experiments H_{ac} (~ 5 mOe) $\ll H_{dc} \ll H_{c2}$ where the excitation field does not modify the average vortex distribution and we can ignore vortex core contribution to λ .

Vortices transmit the perturbation caused by a small AC field as either compressional or tilt waves, depending upon the geometry of the experiment [3]. If the amplitude of the AC field is small, the elastic restoring force is: $F = -\alpha u$, where u is the vortex displacement caused by a small AC current and α is the Labusch parameter. The latter incorporates, self-consistently, both the pinning and the elastic forces. The AC penetration depth is then given by $\lambda^2 = \lambda_L^2 + \lambda_C^2$ where λ_C is the Campbell penetration depth [1–4]. The Campbell length is $\lambda_C = \sqrt{C_{xx}/\alpha}$, where C_{xx} is the appropriate elastic modulus (C_{11} for compression or C_{44} for tilt, $C_{44} \approx C_{11} \approx B^2/4\pi$) [3,4]. Unlike earlier versions based on the local pinning force [1], these formulae are also good approximations for a non-local elastic response with dispersive $\alpha(k)$ [3]. It is also possible to incorporate flux creep and flux flow effects [2–6]. These effects, however, do not result in thermal ir-

reversibility of $\lambda(T, H, j)$. In this paper, we explore the simplest generalization of the elastic model. In the presence of a macroscopic DC Bean current, j , the Lorentz force biases the mean vortex position away from the pinning potential minimum. The Campbell depth is then determined by the small-amplitude response near this new bias point. If the dependence of the pinning potential upon vortex displacement u is non-parabolic, then changes in either j or the critical current j_c will result in changes of the Campbell length. If j relaxes via flux creep or j_c changes with temperature, the Campbell length will then show a small, but observable thermal hysteresis.

Let $V(x)$ describe the shape of the pinning potential with $x = r/r_p$, where r is the vortex displacement and r_p is the effective pinning radius, $r_p \sim \xi$ for a quenched disorder pinning at low temperatures (see Fig. 1). The Lorentz force due to j causes a dimensionless vortex displacement x_0 determined from the condition: $dV/dx = Bj/r_pc = \alpha_0(j/j_c)$, where $\alpha_0 \equiv Bj_c/cr_p$. Upon application of a small AC field, the restoring force acting on a vortex in the vicinity of x_0 is $F(u) \simeq -\alpha u + O(u^2)$ where $u = x - x_0$. It is assumed that j does not change during an AC field cycle. The restoring elastic constant is then $\alpha = d^2V/dx^2|_{x=x_0}$. For a parabolic potential, $\alpha = \alpha_0 = const$ and does not depend on j . For a more general form of the potential we take into account a cubic term in $V(x)$ in the vicinity of x_0 . A Labusch parameter obtained from the Taylor expansion of the restoring force $F = -dV/dx$ around x_0 can be written as $\alpha = \alpha_0(1 - \beta x_0)$, where β is a dimensionless constant. Positive β describes pinning potential $V(x)$ saturating at large x_0 , while negative β corresponds to a potential whose curvature increases with the increase of x_0 . The saturation of a volume pinning force, corresponding to $\beta > 0$, was discussed by Brandt on the

basis of the results of numerical simulations [3]. Saturation also holds for weak collective pinning. A saturating potential provides a smooth crossover to the flux flow regime, where the penetration depth diverges (for zero viscosity). Negative β could be realized for pinning by columnar defects. Assuming $|\beta x_0| \ll 1$ (small deviation of $V(x)$ from parabolic form) we obtain for the vortex displacement due to current j : $x_0 \approx j/j_c$, which gives $\alpha = \alpha_0(1 - \beta j/j_c)$. The linear AC response in the presence of a Bean current j is then described by:

$$\lambda^2(j) \simeq \lambda_L^2 + \frac{\lambda_C^2(0)}{1 - \beta j/j_c} \quad (1)$$

If pinning is weak and magnetic relaxation is fast, as is typical for high- T_c superconductors [6], the term $\beta j/j_c$ is small. Equation (1) then reduces to:

$$\Delta\lambda \equiv \lambda(j) - \lambda(0) = \beta \frac{\lambda_C^2(0)}{2\lambda(0)} \frac{j}{j_c} \quad (2)$$

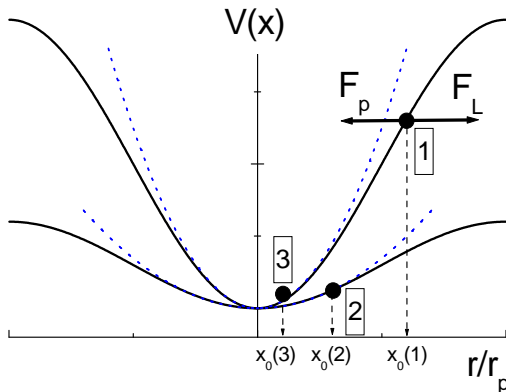


FIG. 1. Schematic illustration of the effective pinning potential. Solid and dotted lines depict non-parabolic and parabolic potentials, respectively. Filled circles represent vortex position in different situations described in the text.

Equations (1) and (2) predict that a non-parabolic potential results in an explicit dependence of λ on j . For a saturating potential ($\beta > 0$), $\lambda(j)$ is predicted to be *larger* than $\lambda(j = 0)$. For a potential in which the curvature increases with x ($\beta < 0$) $\lambda(j)$ would be *smaller* than $\lambda(j = 0)$. Finally, λ should depend upon the *ratio* j/j_c rather than on j alone. We now address each of these three points experimentally and conclude that in typical high- T_c superconductors, $\lambda(j/j_c)$ always *increases* with the increase of a ratio j/j_c thus providing evidence for a saturating pinning potential.

The penetration depth was measured with an 11 MHz tunnel-diode driven LC resonator [7,8] operating in a ^3He refrigerator. An external DC magnetic field (0-7 kOe) was applied using a compensated superconducting magnet. An AC excitation field (~ 5 mOe) was applied parallel to the DC field. For platelet superconducting samples

with both AC and DC magnetic fields applied perpendicular to largest face, an analysis was given in Ref. [8]. When λ is much less than any sample dimension, the resonance frequency shift $\Delta f = f(T) - f(T_{min})$ of the oscillator is proportional to a change in the penetration depth, $\Delta\lambda = \lambda(T) - \lambda(T_{min})$ via $\Delta f = -G\Delta\lambda$, where G is a calibration constant [7,8]. The sample could be moved in and out of the sense coil, thus allowing for both in situ background subtraction and calibration [8]. The noise level, $\Delta f/f_0 \approx 10^{-9}/\sqrt{Hz}$ permitted a resolution of $\Delta\lambda_{ac} \leq 0.5 \text{ \AA}$ for typical samples.

The behavior to be described was observed in a variety of superconducting single crystals including YBaCuO ($T_c \approx 93$ K), BiSrCaCuO ($T_c \approx 90$ K), PrCeCuO ($T_c \approx 21$ K), and (BEDT) organic ($T_c \approx 12$ and 9.5 K) as well as conventional Nb polycrystalline sample ($T_c = 9.27$ K). These properties of the pinning potential persist despite large differences in T_c , symmetry of the order parameter, anisotropy and the sign of charge carriers.

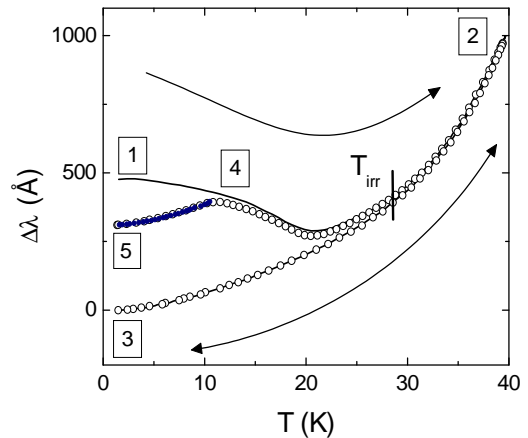


FIG. 2. Curve 1 \rightarrow 2 \rightarrow 3: $H_{dc} = 260$ Oe was applied at $T = 1.5$ K. Then, sample was warmed up and cooled down; Curve 4 \rightarrow 5: field was applied at $T = 12$ K and sample was cooled down; Curve 5 \rightarrow 4 \rightarrow 2 \rightarrow 3: after previous step, sample was warmed up and finally cooled again to $T = 1.5$ K.

Observation of thermal irreversibility: Figure 2 presents a series of temperature sweeps corresponding to different ratios of $j/j_c(T)$ for a BSCCO single crystal. In the first experiment (solid line 1 \rightarrow 2 \rightarrow 3), the sample was cooled in zero field to 1.5 K, a DC field of 260 Oe was applied (after first ramping to -7 kOe to insure complete penetration), and the sample was then warmed (1 \rightarrow 2) and then cooled back to 1.5 K (2 \rightarrow 3). Figure 1 shows the corresponding trajectory of the system in its pinning potential well. Once the temperature exceeded a value $T_{irr}(H)$, $j(t)$ relaxed rapidly and subsequent cooling and warming traces (2 \rightarrow 3 \rightarrow 2) were perfectly reversible. This curve corresponds to motion near bottom of the pinning well where both j and β are small and $\lambda(T)$ reflects changes in $j_c(T)$ or, equivalently, the height of the well.

We refer to the $(2 \rightarrow 3 \rightarrow 2)$ curve as the "reversible" curve. It is identical to that obtained in a direct field-cooled experiment at the same field. $T_{irr}(H)$ represents a vortex "annealing" or low- T irreversibility temperature for the described experiment. In our case, $T_{irr}(260\text{Oe}) = 28\text{ K}$, which is close to the temperature at which several changes in vortex structure are often observed [9]. This temperature is well below the usual irreversibility (and melting) temperature determined from magnetization measurements [9].

The irreversible effects are quite small, $\sim 40\text{ Hz}$ - between marks 1 and 3, Fig. 2. The full frequency shift from the lowest temperature up to T_c is about 10^3 times larger. The same sample, measured using a *Quantum Design* MPMS SQUID magnetometer, showed a diamagnetic Meissner signal of $< 8 \times 10^{-5}\text{ emu}$. Thus, hysteresis in $\lambda(T, j)$ is equivalent to a change in magnetization $\leq 10^{-7}\text{ emu}$. To resolve the shape of a hysteresis curve a sensitivity better than 10^{-8} emu is needed. The effect is even smaller on smaller PCCO samples, where a similar estimation gives $\sim 10^{-9}\text{ emu}$ for the magnitude of the effect. This sensitivity is difficult to achieve in commercial AC susceptometers, but measurements of large ceramic high- T_c samples should, in principle, be able to resolve the irreversibility.

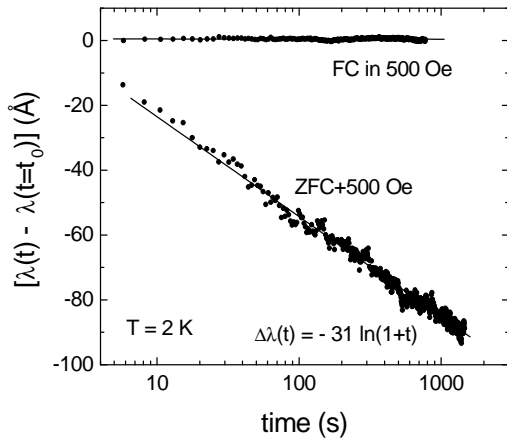


FIG. 3. Time-logarithmic relaxation of the AC penetration depth after application of a 500 Oe magnetic field at 2 K (lower curve) and after FC in 500 Oe (upper curve).

Logarithmic relaxation of $\lambda(j)$: If Eq. (1) is correct, $\lambda(j)$ should relax along with j , due to thermally activated flux creep. Figure 3 shows the time dependence of $\lambda(T, H, t) - \lambda(T, H, t_0)$ at $T = 2\text{ K}$ in BSCCO single crystal. The sample was cooled in zero field, after which $H_{dc} = 500\text{ Oe}$ was applied. Since the temperature was constant $j_c(T)$ did not change but $\lambda(t)$ decreased logarithmically with time. The decrease in $\lambda(t)$ was independent of the sign of j (i.e., if the field was reduced after ramping up to a large value). By contrast, the flat curve shows $\lambda(t)$ after field cooling in 500 Oe to the same temperature. No noticeable relaxation was observed.

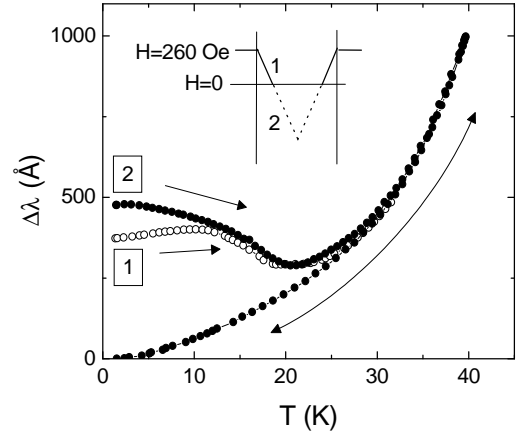


FIG. 4. Curve 1: A 260 Oe magnetic field was applied after ZFC at 1.5 K. Curve 2: After ZFC, magnetic field was first set to -7 kOe and returned back to 260 Oe. Schematics shows corresponding DC profiles of vortex density marked 1 and 2.

Dependence upon j/j_c : In the next experiment, illustrated in Fig. 2, the sample was cooled to $T = 12\text{ K}$ and, after ramping to -7 kOe to ensure a complete flux penetration, a 260 Oe field was applied (point 4 in Fig. 2). The sample was then cooled to 1.5 K (4 \rightarrow 5) and warmed (5 \rightarrow 4 \rightarrow 2) above $T_{irr}(H)$. Again, upon subsequent cooling and warming (2 \rightarrow 3 \rightarrow 2), $\lambda(T)$ remained on the reversible curve and coincided with the reversible curve obtained in the first experiment described above. We interpret this measurement as follows. When a DC magnetic field is turned on at $T_{ZFC} = 12\text{ K}$, j is determined by $U(j/j_c(T)) = T_{ZFC} \ln(\Delta t/t_0)$, where t_0 is the characteristic relaxation time and Δt is the experimental time-window [6]. When the temperature decreases, j_c increases and the activation energy $U(j/j_c)$ increases, thus prohibiting vortices from thermally activated motion and essentially freezing the value of j . If λ were dependent only on j , it would have remained constant from mark 4 to mark 5, Fig. 2. The fact that it decreases implies a parametric change in the pinning potential: when j_c increases, j/j_c decreases and by Eq. 1, the Campbell length decreases. When the temperature is again increased (5 \rightarrow 4) $j(T)$ remains frozen at its value originally set at T_{ZFC} (mark 4) and $\lambda(T)$ retraces the preceding cooling (4 \rightarrow 5) curve reversibly. Above $T_{ZFC}\text{ K}$, the activation energy $U(j/j_c)$ becomes low enough for j to once again relax. Then, $\lambda(T)$ decreases until contribution of the reversible curve becomes dominant.

Tilt contribution to the signal, λ_{44} : In the configuration used here (magnetic field normal to the conducting planes of a thin platelet), the magnetic field penetrates both from sides and from the top and bottom surfaces. In the Meissner state, this was demonstrated by solving numerically the London equation and testing the results experimentally [8]. In the presence of vortices, penetration from sides, λ_{11} , is mediated by compressional waves,

whereas penetration from the top and bottom faces is due to tilt waves, λ_{44} [3]. For thin enough samples, the latter contribution must dominate the former as we now show experimentally. In Fig. 4, the sample was zero-field cooled to $T = 1.5$ K and a 260 Oe magnetic field, less than a field of full penetration, was applied (mark 1 in Fig. 4). This produced a partially-penetrated state where only a fraction of the sample interior was filled with vortices, as illustrated by solid lines in the Bean profile shown in Fig. 4. Upon warming, j decreased and vortices filled the sample. If most of the signal comes from the top and bottom surfaces, the penetration depth must increase as vortices fill the sample. Only when vortices reach the sample center should the signal decrease in accordance with Eq.(1). Exactly this behavior was observed on the curve starting at point 1 in Fig. 4. The sample was then cooled from above T_c in zero field to 1.5 K. H was then ramped down to -7 kOe and then returned back to +260 Oe, producing the fully penetrated state shown by the dotted and solid lines in Fig. 4. The resulting curve beginning at 2 is shown in Fig. 4. $\lambda(T)$ decreased monotonically upon warming, indicating that tilt motion of vortices penetrating the top and bottom surfaces constituted the primary signal contribution.

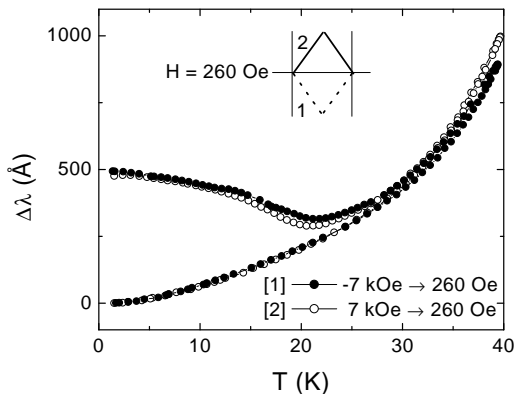


FIG. 5. Comparison of $\Delta\lambda(T)$ for flux entry and exit. **Closed symbols:** magnetic field was ramped up from -7 kOe to +260 Oe (flux entry). **Open symbols:** field was ramped down from +7 kOe to +260 Oe (flux exit) and the sample was warmed-then-cooled. Schematics shows the corresponding profiles of vortex density.

Although the Campbell length in a uniform state depends upon B , the observed hysteresis depends explicitly upon j/j_c . (A weak implicit B -dependence may arise through $j/j_c(B)$). This fact is demonstrated in Fig. 5 where we compare $\lambda(T)$ measured at the same final value of applied field, $H = 260$ Oe applied at 1.5 K. The solid symbols correspond to the initial application of a -7 kOe magnetizing field while the open ones correspond to +7

kOe magnetizing field. Both fields were then ramped to $H = +260$ Oe before measurements began. These field changes were sufficient for full flux penetration. The corresponding flux profiles are shown schematically in Fig. 5. The value of B throughout the sample was much different for these two starting conditions, but the thermal hysteresis curves are essentially identical, demonstrating that the hysteresis in λ_C is directly related to j/j_c , not B . The small differences at elevated temperatures could be attributed to the differences in $j/j_c(B)$.

In conclusion, we have demonstrated that thermal hysteresis of the AC penetration depth can be attributed to changes in j/j_c according to Eq.(1). The effect is observable only for a non-parabolic pinning potential that, as follows from our measurements, saturates with displacement. We identify a new low temperature irreversibility line above which thermal hysteresis vanishes. A comprehensive study of $T_{irr}(H)$ in conventional and layered superconductors will be presented in a forthcoming paper.

Acknowledgments: We thank V. Geshkenbein, A. Koshelev, V. Vinokur, A. Gurevich, J. R. Clem and E. H. Brandt for useful discussions and communications. Work at UIUC was supported by Science and Technology Center for Superconductivity Grant No. NSF-DMR 91-20000. Work at The University of Tokyo is supported by CREST and Grant-in-Aid for Scientific Research from the Ministry of Education, Science, Sports and Culture of Japan. Work at Argonne National Lab supported by U.S. DOE-BES Contract No. W-31-109-ENG-38 and NSF-STCS Contract No. DMR 91-20000.

- [1] A. M. Campbell and J. E. Evetts, "Critical currents in superconductors" (Taylor & Francis Ltd., London, 1972).
- [2] M. W. Coffey and J. R. Clem, Phys. Rev. Lett. **67**, 386 (1991); M. W. Coffey and J. R. Clem, Phys. Rev. B **45**, 10527 (1992).
- [3] E. H. Brandt, Phys. Rev. Lett. **67**, 2219 (1991); E. H. Brandt, Physica C **195**, 1 (1992); E. H. Brandt, Rep. Prog. Phys. **58**, 1465 (1995).
- [4] A. E. Koshelev and V. M. Vinokur, Physica C **173**, 465 (1991).
- [5] C. J. van der Beek, V. B. Geshkenbein, V. M. Vinokur, Phys. Rev. B **48**, 3393 (1993).
- [6] G. Blatter, M. V. Feigelman, V. B. Geshkenbein, A. I. Larkin, and V. M. Vinokur, Rev. Mod. Phys. **66**, 1125 (1994).
- [7] C. T. Van Degrift Rev. Sci. Inst. **46**, 599 (1975); A. Carrington *et. al.*, Phys. Rev. B **59**, R14173 (1999).
- [8] R. Prozorov, R. W. Giannetta, A. Carrington, and F. M. Araujo-Moreira, cond-mat/0003003.
- [9] P. H. Kes *et. al.*, J. Phys. I France **6**, 2327 (1996).